The EMBO Journal Vol. 22 No. 18 pp. 4656–4665, 2003

Direct imaging of lateral movements of AMPA receptors inside synapses

Catherine Tardin[1,2], Laurent Cognet[1], Cécile Bats[2], Brahim Lounis[1] and Daniel Choquet[2,3]

[1]Centre de Physique Moléculaire Optique et Hertzienne – CNRS UMR 5798 et Université Bordeaux 1, 351 Cours de la Libération, 33405 Talence and [2]Laboratoire de Physiologie Cellulaire de la Synapse – CNRS UMR 5091 et Université Bordeaux 2, Institut François Magendie, 1 rue Camille Saint-Saëns, 33077 Bordeaux, France

[3]Corresponding author
e-mail: dchoquet@u-bordeaux2.fr

C.Tardin and L.Cognet contributed equally to this work

Trafficking of AMPA receptors in and out of synapses is crucial for synaptic plasticity. Previous studies have focused on the role of endo/exocytosis processes or that of lateral diffusion of extra-synaptic receptors. We have now directly imaged AMPAR movements inside and outside synapses of live neurons using single-molecule fluorescence microscopy. Inside individual synapses, we found immobile and mobile receptors, which display restricted diffusion. Extra-synaptic receptors display free diffusion. Receptors could also exchange between these membrane compartments through lateral diffusion. Glutamate application increased both receptor mobility inside synapses and the fraction of mobile receptors present in a juxta-synaptic region. Block of inhibitory transmission to favor excitatory synaptic activity induced a transient increase in the fraction of mobile receptors and a decrease in the proportion of juxtasynaptic receptors. Altogether, our data show that rapid exchange of receptors between a synaptic and extra-synaptic localization occurs through regulation of receptor diffusion inside synapses.

Keywords: glutamate receptors/lateral diffusion/single-molecule fluorescence microscopy/synaptic transmission

Introduction

AMPA glutamate receptors (AMPARs) are ligand-activated cation channels concentrated in the postsynaptic density (PSD) that mediate fast excitatory neurotransmission in the CNS (Dingledine *et al*., 1999). Concentration of AMPARs at PSDs is thought to result from their stabilization by interactions with specific intracellular scaffolding proteins and cytoskeletal elements (Braithwaite *et al*., 2000; Nusser, 2000; Scannevin and Huganir, 2000). AMPARs constitutively cycle in and out of the postsynaptic membrane at a rapid rate through endo- and exocytosis. The regulation of the balance between these processes may account for the rapid variations in receptor composition of the PSD during synaptic plasticity (reviewed in Carroll *et al*., 2001; Malinow and Malenka, 2002; Sheng and Kim, 2002). A simplified scheme would be that postsynaptic LTP involves increased exocytosis of AMPARs, while LTD would be underlied by increased endocytosis of receptors.

Recently, a role for receptor diffusion within the plasma membrane has been suggested in AMPARs trafficking in and out of PSDs. First, GluR2 containing AMPARs diffuse rapidly in the extra-synaptic membrane and stop reversibly in the periphery of synapses (Borgdorff and Choquet, 2002). Secondly, endo- or exocytosis may occur at the periphery of synapses rather than directly at PSDs. For endocytosis, clathrin assembly occurs at hotspots laterally to the PSDs (Blanpied *et al*., 2002). LTD or glutamate application trigger an increase in the amount of endocytosed AMPARs (Carroll *et al*., 1999a,b; Beattie *et al*., 2000; Wang and Linden, 2000). Endocytosis of AMPARs may first require their dispersal from the synaptic to the extrasynaptic membrane through lateral diffusion, as glutamate by itself does not increase the efficiency of the endocytotic pathway (Zhou *et al*., 2001). Reciprocally, whether there are also hotspots for exocytosis of receptors outside of the PSD is unknown. At early times after exocytosis, new GluR1 subunits are diffusively distributed along dendrites. This is followed by their lateral translocation and accumulation into synapses (Passafaro *et al*., 2001). Delivery of receptors to the PSD after exocytosis may thus also involve diffusion.

Mechanisms involved in the regulation of the accumulation of AMPARs at synaptic sites through lateral diffusion are emerging. Local increases in intracellular calcium drastically reduce AMPAR diffusion rate (Borgdorff and Choquet, 2002). Stargazin, a protein that links AMPARs to PSD-95, might regulate AMPAR trafficking between the synaptic and extra-synaptic membrane (Schnell *et al*., 2002). Therefore, it is likely that diffusion of receptors in the plane of the membrane is necessary for their removal or addition to and from the PSD, although this has never been visualized directly.

If receptors enter and leave synapses through lateral diffusion, they have to unbind from the postsynaptic scaffold, diffuse through the PSD and exit the synapse. Clusters of receptors mimicking the PSD can be induced in the synaptic and extra-synaptic membrane by co-expression of scaffold and receptor molecules. At the extra-synaptic clusters, we had directly visualized entry and exit of receptors from the clusters at high rates using single particle tracking (Meier *et al*., 2001; Sergé *et al*., 2002). However, the size of the particle (500 nm) precluded tracking of receptors inside the synaptic cleft.

In this study, we use the single-molecule fluorescence imaging approach (e.g. Schmidt *et al*., 1995; Dickson *et al*., 1996; reviewed in Moerner and Orrit, 1999; Weiss, 1999) to localize and track GluR2-containing AMPA receptors inside synaptic sites below the optical diffraction limit. We

Published by Oxford University Press

show that a large proportion of AMPARs diffuse inside synapses and that this diffusion is regulated during protocols that modify receptor accumulation at synapses. We propose that receptor disappearance from postsynaptic sites involve their dispersal through increased lateral diffusion while receptor accumulation involves their delayed stabilization after diffusion.

Results

Single molecule imaging in live neurons

Anti-GluR2 antibodies were labeled with Cy5 or Alexa-647 molecules at low labeling ratio (mean labeling ratio of 0.4 dye per antibody) so that individual antibodies were labeled at most with one fluorophore. A small proportion of surface expressed AMPA receptors containing the GluR2 subunit were selectively labeled in live neurons through short incubations with these antibodies. We could thus image and resolve discrete fluorescence spots with an epifluorescence imaging setup (Schmidt *et al*., 1995; Dickson *et al*., 1996). The majority of the fluorescence spots (75 ± 6%, n = 80 neurons) exhibit one-step photobleaching (Figure 1E; Supplementary movies 1–4, available at *The EMBO Journal* Online) and not a gradual decay as for ensemble photobleaching. The width of these spots corresponds to the point-spread function of the microscope and the signal originating from them ranges from 500 to 1000 counts per 30 ms. Thus, these fluorescence spots have all the hallmarks of individual fluorescent molecules (see Supplementary figure 1; reviewed in Moerner and Orrit, 1999; Weiss, 1999) bound to GluR2 receptors. Only these spots were thus retained for analysis. The imaged single molecules were optically well resolved (Figure 1C; Supplementary movies 1–4) and their density on the cell surface was much less than 1/μm^2. This indicates that antibody incubation did not result in cross-linking of more than two GluR2-containing AMPARs, the anti-GluR2 being bivalent. This was further supported by immunocytochemistry experiments: the apparent level of receptor clustering was smaller when incubation with anti-GluR2 was performed on live compared with fixed cells (percentage of clustered receptors 15 ± 7%, n = 12, and 23 ± 9%, n = 12, respectively). However, this does not rule out the possibility that single molecule tracking follows the movement of a natural cluster of receptors, only one receptor being labeled.

Trajectories of such molecules were reconstructed from image series recorded at a rate of 33 Hz (see movies in Supplementary data). The length of the trajectories varied from 0.1 to 0.5 s up to 4 s, depending on the photobleaching time of the molecule (mean ± SD 244 ± 318 ms, n = 3078 molecules). The mean-square displacement (MSD) corresponding to trajectories of individual fluorescent molecules dried on glass shows that individual molecules are pointed within 45 ± 5 nm accuracy (Schmidt *et al*., 1995; Thompson *et al*., 2002) (Figure 2B, trajectory 1).

GluR2 molecules are imaged in synapses

We first analyzed the spatial distribution of AMPARs with respect to synaptic sites in bulk immunocytochemistry experiments and at the single molecule level in live neurons. For both types of experiments, live neurons were incubated for short periods with anti-GluR2 antibodies (10 min). For bulk visualization of receptors only, this step was followed by fixation and amplification of the signal through secondary antibodies. In immunocytochemistry experiments, AMPARs accumulated in front of glutamatergic presynaptic terminals specifically stained by the vesicular glutamatergic transporter BNPI/VGLUT1 (Figure 1F). A similar accumulation was previously observed using other presynaptic markers (Carroll *et al*., 1999b; Noel *et al*., 1999). In live neurons, presynaptic terminals were stained with FM1-43 or rhodamine 123 (Figure 1B; Supplementary movies 2–4). We measured the distance r between each individual AMPARs and the center of the closest stained synaptic site. We plotted $S(r)$, the proportion of individual molecules per unit surface, as a function of r (Figure 1G). Individual AMPARs are strongly enriched (~10 times) at and close to (<300–400 nm) synaptic sites. Altogether, these experiments indicate that synaptic AMPARs can be stained through incubation with antibodies in live neurons. They further establish that live staining of presynaptic terminals is a valid approach to discriminate between synaptic and extra-synaptic regions and analyze AMPAR movements in these membrane domains.

Diffusion characteristics are correlated with localization with respect to synapses: examples

Single molecule trajectories were initially sorted into two main categories: the first one corresponds to molecules located at a distance <300 nm from the center of a presynaptic staining and are referred to as 'synaptic' throughout this work using this cut-off criterion (see Materials and methods). Three of these trajectories are illustrated by examples 2 and 3 in Figure 2A, and in Supplementary movie 4. The second group category corresponds to all the others, including molecules found in the periphery of synapses. They are referred to as 'extra-synaptic' and illustrated by example 4 in Figure 2A, and in Supplementary movies. We observed a variety of mobility behaviors for the receptors, which are correlated with the localization. They ranged from highly mobile receptors only seen in extra-synaptic regions (exemplified by trajectory 4 in Figure 2A) to mildly mobile (trajectory 3) or immobile (trajectory 2). The latter two were mainly found at synaptic sites. Strikingly, individual receptors directly entering and leaving synaptic domains could be observed on occasion (~1–2% of all trajectories; e.g. trajectory 5 in Figure 2A, and Supplementary movie 2).

The MSD is widely used to extract diffusion characteristics from trajectories. In Figure 2B, the MSD is plotted as a function of time for trajectories 1–4 illustrated in Figure 2A. The extra-synaptic mobile receptor diffused freely, as indicated by its linear MSD, while the movement of mobile receptors in synapses was confined to a domain, as indicated by the plateau reached by its MSD over time. The domain size was typical for a synapse (~400 nm; see below).

Diffusion characteristics are correlated with localization with respect to synapses: statistical and analytical analysis

We performed a statistical analysis on the mobility of AMPARs in each region (synaptic or extra-synaptic). We

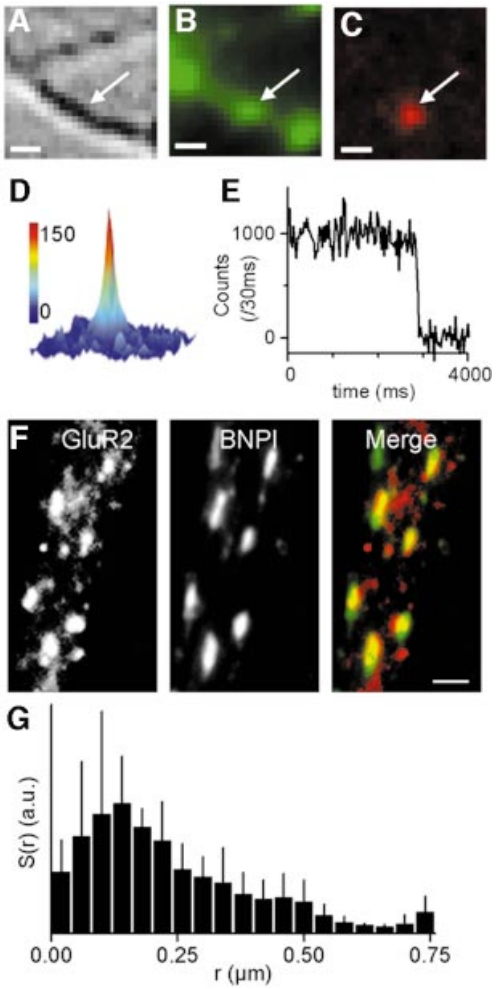

Fig. 1. Single-molecule fluorescence detection of GluR2-containing AMPARs. (**A**–**C**) Simultaneous images of a neurite of a living neuron as seen by differential interference contrast (A) and epifluorescence of FM1-43 on a green channel and Cy5 on a red channel (B, C). (B) Synaptic sites stained by depolarization-induced uptake of FM1-43. (C) Diffraction limited spot image of a single Cy5-anti-GluR2 antibody. The molecule is co-localized with one of the three synaptic sites of (B) (see also Supplementary movies). Scale bar = 1 µm. (**D**) Three-dimensional representation (intensity in the vertical axis) of the fluorescence of the molecule in (B). Scale bar is counts per 30 ms. (**E**) Recording of the fluorescence intensity of a single Cy5-anti-GluR2 molecule over time displaying the characteristic one-step photobleaching. (**F**) Double staining of surface GluR2 on a live neuron (left and red in the merge) and presynaptic terminals with an anti-vesicular glutamate transporter (middle and green in the merge). (**G**) Surface proportion of the detected AMPARs $S(r)$ (see text) for single molecules recorded in the presence of TTX. AMPARs accumulate at and close to synaptic staining maxima.

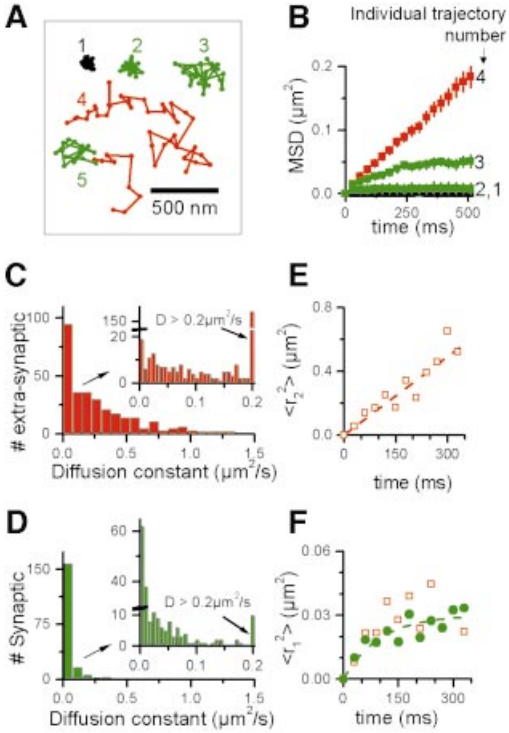

Fig. 2. (**A** and **B**) Illustrative examples of AMPARs movements. (A) Examples of trajectories of individual molecules. Cy5-anti-GluR2 fixed on a coverslip (1). The other trajectories correspond to single Cy5-anti-GluR2 bound to AMPARs in living dendrites. The trajectories recorded in synaptic regions (see text) are indicated in green. The trajectories recorded in extra-synaptic domains are indicated in red. Trajectories 2 and 3 stayed within synaptic sites; trajectory 4 evolved entirely in the extra-synaptic membrane; trajectory 5 started in an extra-synaptic region and then entered a synaptic site. (B) Plots of the MSD versus time intervals τ for four trajectories shown in (A). Trajectories 2 and 3, which were both synaptic, were less mobile than trajectory 1, but differed: trajectory 2 corresponds to a slowly mobile receptor in a confined area, 3 to an immobile receptor. (C–F) Statistical analysis of AMPAR movements. (C and D) Differential mobility of synaptic and extra-synaptic AMPARs measured at 37°C in the presence of TTX. (**C**) Histograms of the instantaneous diffusion constant for 306 AMPARs trajectories detected in extra-synaptic regions of >20 neurons. (**D**) Same histograms for 187 AMPARs trajectories detected in synaptic sites of >20 neurons. Binning of the major histograms is 0.075 µm²/s. The insets correspond to the same data with a binning of 0.007 µm²/s. (E and F) Single-molecule analysis of AMPARs diffusion: plots of the mean MSD $<r^2_1(\tau)>$ and $<r^2_2(\tau)>$ derived from the analysis of the square displacements for $\tau = n \times 30$ ms (n = 1–11). (**E**) $<r^2_2(\tau)>$ is linear with time and reveals free diffusion for fast diffusing extra-synaptic AMPARs. (**F**) $<r^2_1(\tau)>$ are undistinguishable for synaptically located (filled circle) and slowly diffusing extra-synaptic (open squares) trajectories and reveal confined movement.

first analyzed the trajectories of AMPARs in the presence of TTX to block spontaneous neuronal activity (the examples shown in Figure 2A and B were part of 493 trajectories from more than 20 different neurons recorded at 37°C). After sorting the 493 trajectories with respect to their localizations in the two regions, we calculated the instantaneous diffusion coefficient, D, for each trajectory, from linear fits of the first three to five points (corresponding to 90–150 ms) of the MSD (Kusumi *et al.*, 1993; Sergé *et al.*, 2002) using: MSD $(\tau) = < r^2 > (\tau) = 4D\tau$.

Distributions of D for synaptic and extra-synaptic receptors were strikingly different (Figure 2C and D), synaptic receptors diffusing more slowly than extra-synaptic ones. In the extra-synaptic region, we distinguished three populations from the histograms (Figure 2C). For the majority (66%) of the molecules, the diffusion coefficient was in the range of 0.1–1 µm²/s (mean ± SEM 0.45 ± 0.05 µm²/s, n = 202 trajectories, seven experiments) in good agreement with measurements made by single particle tracking (Borgdorff and Choquet, 2002). The two other populations correspond to molecules which were either immobile (8%, D $<7 \times 10^{-3}$ µm²/s, n = 25) or diffused slowly (26% with D <0.1 µm²/s, mean 0.05 ± 0.01 µm²/s, n = 82; see inset in Figure 2C). In stained synaptic sites, receptors could be separated into two populations (Figure 2D). Half of the receptors were immobile, whereas the other half diffused with a diffusion

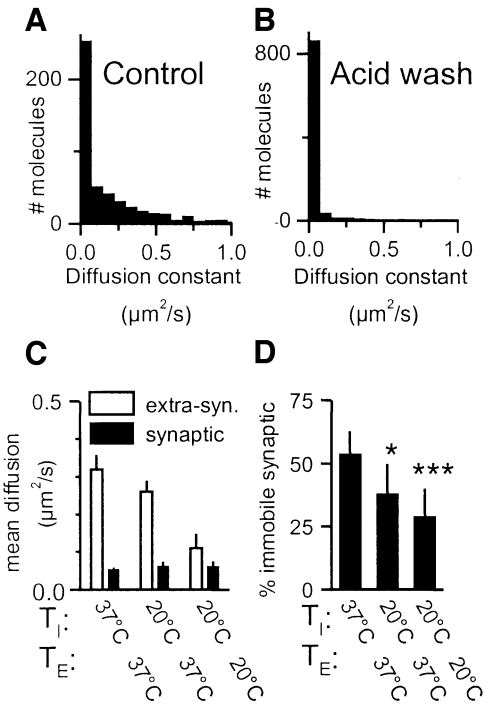

Fig. 3. (**A** and **B**) Histograms of the cumulative distribution of instantaneous diffusion constant of synaptic and extra-synaptic receptors in control conditions (A) and after acid wash to detect specifically endocytosed AMPARs (493 and 975 trajectories, respectively). Binning as in Figure 2C. (C and D) Temperature dependence of AMPAR diffusion. (**C**) Mean instantaneous diffusion constant for freely diffusing AMPARs in extra-synaptic regions (hollow) and for diffusing AMPARs (with restricted diffusion) at synaptic sites (filled) as a function of T_I and T_E, the incubation temperatures during the labeling by anti-GluR2, T_I, or during the experiments, T_E. (**D**) Fraction of immobile over mobile receptors in synaptic sites for different temperatures.

coefficient between 1.5×10^{-2} and 0.1 μm²/s (mean 0.054 ± 0.005 μm²/s, $n = 100$). At a given location (synaptic or extra-synaptic), AMPARs with different mobilities were found. In particular, both mobile and immobile receptors were observed successively at the same synaptic site within the same recording sequence in 21 cases, showing that the two receptor's behaviors do not arise from receptors present in separate types of synapses. Moreover, these observations show that on the time scale of our experiments, the movement of synaptic AMPARs is not that of the whole PSDs.

In order to analytically characterize the diffusion properties of each subpopulation at each location, we used a second approach based on the distribution of the squared displacements of the molecules (Schuetz *et al*., 1997). This approach allows us to unravel and analyze multiple diffusion types in each compartment without having to classify the MSDs of the individual molecules, thus avoiding possible bias by an arbitrary sorting. As a result, three categories of receptor movements were also found by this analytical analysis (see Supplementary figure 2), characterized by the time dependence of their mean MSD, $<r_i^2(\tau)>$, where $i = 0$–2. Fast mobile receptors ($i = 2$) were exclusively found in extra-synaptic regions, while the slowly mobile ($i = 1$) and immobile ($i = 0$) receptors were mainly found in synaptic domains (Figure 2E and F; Supplementary data). Thus, two independent analysis protocols, i.e. distributions of individual D values (Figure 2C and D) and distributions of squared displacements (Supplementary figure 2; Figure 2E and F), establish the existence of different receptor populations in terms of mobility. Moreover, the latter analysis paradigm establishes the type of diffusion for the two mobile populations. On one hand, $<r_2^2(\tau)>$ is linear with time, indicating that these extra-synaptic receptors undergo free Brownian diffusion (at least up to 330 ms; Figure 2E) with a mean diffusion constant of 0.37 ± 0.04 μm²/s. On the other hand, $<r_1^2(\tau)>$ saturates with time (Figure 2F), a signature of spatially restricted diffusion (Kusumi *et al*., 1993; Sergé *et al*., 2002). These were found, with very similar properties, in both the synaptic and extra-synaptic receptor populations, although in different proportions ($45 \pm 5\%$ for synaptic and $25 \pm 5\%$ for extra-synaptic receptors; data not shown). The diffusion coefficient D_1 and the diameter L of the domain within which diffusion is restricted can be derived (Kusumi *et al*., 1993) from:

$$\langle r_1^2(\tau)\rangle = \frac{L^2}{3}\left(1 - \exp\left(\frac{-12D_1\tau}{L^2}\right)\right) \qquad (17)$$

Least-square fitting of the data by Equation 1 gives $D_1 = 6 \pm 2 \times 10^{-2}$ μm²/s and a domain size $L = 300 \pm 20$ nm. The domain size is in good quantitative agreement with the synaptic sizes given by electron microscopy (Schikorski and Stevens, 1997; Takumi *et al*., 1999), suggesting that mobile receptors explore the whole postsynaptic domain. Receptors that we labeled as extra-synaptic and which nevertheless displayed restricted diffusion could in fact pertain to unstained synapses. Alternatively, we have previously shown that extra-synaptic receptors aggregated by scaffolding proteins display a similarly restricted mobility (Meier *et al*., 2001; Sergé *et al*., 2002).

Contribution of endocytosis to receptor mobility

GluR2 containing AMPARs are known to undergo continuous endo/exocytosis and recycling (Carroll *et al*., 2001). Our experiments did not detect newly exocytosed receptors as no free antibody was present during the recordings. In contrast, antibodies are known to be endocytosed together with the receptors to which they are bound (e.g. Luscher *et al*., 1999). We first measured by imunohistochemistry on live cells the global level of endocytosis of antibody-tagged receptors. Neurons were incubated 10 min with anti-GluR2 at 37°C, washed, and further incubated 15 min at 37°C before being fixed and stained for surface and endocytosed receptors (see Materials and methods). We found that $24 \pm 5\%$ (mean ± SEM, 11 neurons) of the receptors were endocytosed in neurites. Then, to investigate specifically the mobility of endocytosed receptors, we first incubated labeled cells for 30 min at 37°C to allow endocytosis to occur, then removed surface labeling by acid wash prior to performing single molecule experiments. Surface staining was decreased by $80 \pm 9\%$ ($n = 10$ neurons) by this treatment. The mobility of the internalised receptors is shown Figure 3. We found that after acid wash, 79% of the

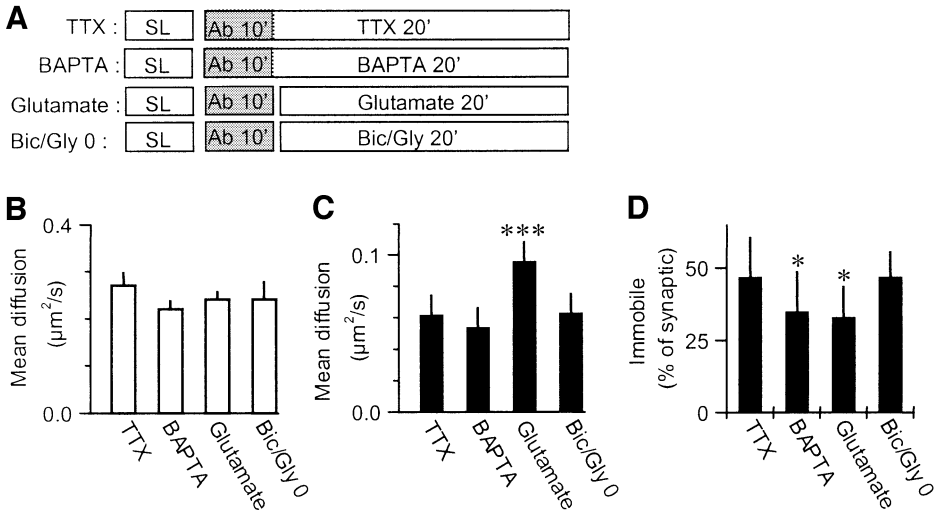

Fig. 4. Regulation of AMPARs mobility in conditions of synaptic plasticity. (**A**) Protocols: synapse labeling (SL) is followed by antibody incubation for 10 min at 20°C (Ab) before single molecule experiments at 37°C for 20 min in the presence of different pharmacological agents. (**B**) Mean diffusion constants for mobile extra-synaptic AMPARs in the four conditions (n = 356/10, 606/16, 627/15 and 578/21 trajectories/experiments for respectively TTX, BAPTA, Glutamate and Bic/Gly applications). No significant difference is detected. (**C**) Mean diffusion constants (± SD) for mobile synaptic AMPARs in the four conditions. Glutamate induces a 55% increase in the mobility of the synaptic AMPARs ($P < 0.001$ that the Glut value is different from the three others, Student's t-test; n = 177/10, 60/16, 169/15 and 54/21 trajectories/experiments for, respectively, TTX, BAPTA, Glutamate and Bic/Gly applications). (**D**) Fraction of immobile over mobile receptors in synaptic sites for the four different conditions showing a slight but significant decrease of the proportion of immobile synaptic AMPARs during glutamate or BAPTA application ($P < 0.05$ that the BAPTA and Glutamate value are different from the two others, Student's t-test).

total receptors (synaptic plus extra-synaptic) were immobile, compared with 25% in control recordings.

To further investigate the contribution of receptor endocytosis to the proportion of immobile receptors, we performed temperature block of endo/exocytosis in the presence of TTX. First, in immunohistochemistry experiments, we found that the percentage of endocytosis after 15 min at 20°C dropped to 10 ± 4% (eight neurons). Secondly, 433 (respectively 422) single-molecule trajectories from 20 different live neurons were recorded at 37°C (respectively 20°C) after antibody incubation at 20°C to reduce the amount of internalized receptors. The mean diffusion constants of the mobile population of receptors in synaptic sites was not different between 37 and 20°C (Figure 3C); however, it decreased by a factor of three at 20°C in the extra-synaptic regions (including all mobile extra-synaptic receptors it varied from 0.32 ± 0.04 µm²/s, n = 207 at 37°C to 0.11 ± 0.04 µm²/s, n = 82 at 20°C). This shows that diffusion of receptors at synaptic sites is not limited by the viscosity of the membrane, as it is likely to be in extra-synaptic regions. This decrease in diffusion constants in extra-synaptic regions led to an apparent 2-fold increase in the proportion of receptors counted as immobile ($D < 7.10^{-3}$ µm²/s; data not shown). In contrast, as the mean diffusion of receptors in the synaptic regions did not change with temperature, we could directly compare the evolution in the proportion of immobile receptors. It decreased by >40% when going from 37 to 20°C (see Figure 3D). This decrease is larger than what could be expected from a simple block of endocytosis and may arise from additional phenomena. In any case, this confirms that endocytosed receptors belong to the immobile population. All data presented below were obtained from recordings performed at 37°C after antibody incubations at 20°C.

Regulation of AMPARs mobility inside synapses

Postsynaptic plasticity of glutamatergic synapses is mediated in large part by the regulation of AMPAR trafficking (reviewed in Carroll *et al.*, 2001; Malinow and Malenka, 2002; Sheng and Kim, 2002). Protocols that induce plasticity of synaptic transmission in culture result in changes of AMPAR concentration at synapses and are thought to mimic at the molecular level the processes of LTP and LTD (Carroll *et al.*, 1999a; Beattie *et al.*, 2000; Lin *et al.*, 2000; Lu *et al.*, 2001; Passafaro *et al.*, 2001). Changes in AMPAR numbers at synapses have mainly been attributed to changes in endocytosis or exocytosis of receptors. These membrane traffic events are likely to occur outside PSDs (Passafaro *et al.*, 2001; Blanpied *et al.*, 2002), which implies that receptor diffusion in the plane of the plasma membrane should participate to the changes in synaptic receptor numbers. Here, we analyze whether AMPARs diffusion inside and outside synapses is regulated by glutamate application and changes in synaptic activity.

We used bath application of glutamate to decrease the number of surface-expressed AMPARs (Carroll *et al.*, 1999a; Beattie *et al.*, 2000) through mechanisms that may be shared by LTD (Carroll *et al.*, 1999b; Man *et al.*, 2000). This protocol is referred herein as 'Glut'. Conversely, we also used activation of synaptic release of glutamate through blocking inhibitory neurotransmission by biccuculine and strychnine, together with potentiation of NMDARs by glycine to increase the number of surface AMPARs through mechanisms that may be similar to those of LTP (Lu *et al.*, 2001; Passafaro *et al.*, 2001). This protocol is referred herein as 'Bic/Gly'. Our control condition was, as previously, recordings in the presence of TTX. As a further resting condition, we also used intracellular BAPTA to chelate pre- and postsynaptic intracellular calcium.

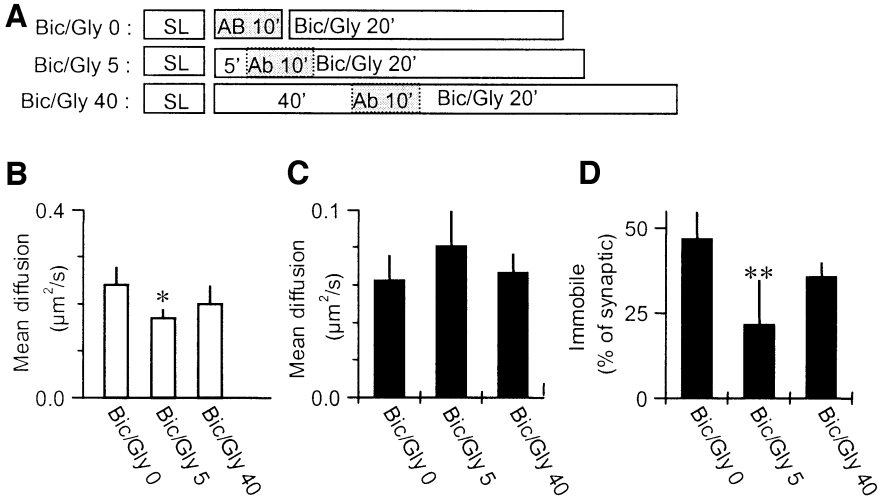

Fig. 5. Transient regulation of AMPARs mobility in conditions of Bic/Gly bath application. (**A**) Protocols: the fourth protocol shown in Figure 4A is modified by delaying the antibody incubation either 5 or 40 min after bath application of biccuculine, strychnine and glycine (Bic/Gly). (**B**) Mean diffusion constants for mobile extra-synaptic AMPARs in the three conditions. (**C**) Mean diffusion constants for mobile synaptic AMPARs in the three conditions. (**D**) Fraction of immobile over mobile receptors in synaptic sites for the three conditions showing a transient decrease of the proportion of immobile synaptic AMPARs at 5 min after Bic/Gly treatment ($P < 0.01$ that the Bic/Gly5 is different from the two others, Student's *t*-test; $n = 54/21$, 64/29 and 70/15 trajectories/experiments for, respectively, Bic/Gly0, Bic/Gly5 and Bic/Gly40).

We first verified by immunohistochemistry on live neurons (data not shown) that these protocols induced reciprocal changes in surface expression of AMPARs (Carroll *et al*., 1999a; Beattie *et al*., 2000; Lin *et al*., 2000; Lu *et al*., 2001; Passafaro *et al*., 2001). Indeed, bath application of 100 μM glutamate induced a 85% increase in the percentage of endocytosed AMPARs within 15 min. This corresponded to a loss of 22% of the surface receptors. Bath application for 5 min of 20 μM biccuculine and 1 μM strychnine together with 200 μM glycine induced a 59% increase (SD 19%, $n = 10$) in surface AMPARs. We then studied the effect of these protocols on receptor mobility at the single molecule level. In a first series of experiments, we labeled surface receptors at 20°C for 10 min and applied the different pharmacological agents during the recordings (Figure 4A). The diffusion of extra-synaptic receptors was not significantly modified by these treatments (Figure 4B). In contrast, bath glutamate induced a strong (55%) increase of the mean diffusion constant of AMPARs inside synapses (Figure 4C). This was accompanied by a 30% reduction in the proportion of immobile synaptic receptors (Figure 4D). This is surprising, since glutamate promotes AMPARs endocytosis and endocytosed receptors are mostly immobile (Figure 3B). A tempting explanation for this discrepancy is that glutamate treatment induces the accumulation of endocytotic vesicles mainly in the cell body rather than in neurites, as previously published (data not shown; Beattie *et al*., 2000). Intracellular BAPTA decreased by 30% the percentage of immobile synaptic receptors, in accordance with the BAPTA-induced decrease in AMPARs stabilization reported previously (Borgdorff and Choquet, 2002). We found no effect on either parameters of the of Bic/Gly protocol compared with the control TTX condition.

We observed no effect of the Bic/Gly treatment. Indeed, in Figure 4, receptor labeling was performed before the Bic/Gly application, thus newly inserted receptors were not labeled. Furthermore, previous studies have indicated that upon this type of treatment, receptors might be first exocytosed outside synapses and accumulated at synapses with a delay (Passafaro *et al*., 2001). We thus delayed the labeling of the receptors to 5 and 40 min after application of Bic/Gly and then studied their mobility (Figure 5). The diffusion coefficients of synaptic or extra-synaptic receptors did not vary much in these different conditions (Figure 5B and C). In contrast, we found a strong transient reduction after 5 min of Bic/Gly treatment in the proportion of immobile synaptic receptors (Figure 5D). Newly inserted receptors are thus initially diffusive and then stabilized at synaptic sites.

Regulation of receptor localization near synapses

During glutamate application, we qualitatively observed a large number of highly mobile molecules right next to synapses. We thus quantified the localization of receptors in the various conditions and compared their distributions. The distribution $S(r)$ of receptors in the presence of bath applied glutamate shown in Figure 6A, was compared (Figure 6B) with the control one previously shown on Figure 1G. In the presence of glutamate, we indeed found a strong increase in the proportion of receptors present in the periphery of synapses, in an annulus ~400–800 nm from the center of the synapses. The mobility of these juxtasynaptic AMPARs ($D = 0.24 \pm 0.02$ μm²/s) is however not different from that of the other extra-synaptic receptors ($D = 0.25 \pm 0.02$ μm²/s). We compared the mean percentage of receptors present in this juxtasynaptic annulus in the different conditions studied above (Figure 6D). In the presence of glutamate, the proportion of juxtasynaptic AMPARs was twice that observed under TTX. No significant change in this proportion was observed in the presence of BAPTA or for 0 or 5 min of Bic/Gly treatment. Strikingly, we found a 40% reduction decrease in the proportion of juxtasynaptic receptors after 40 min of Bic/Gly treatment.

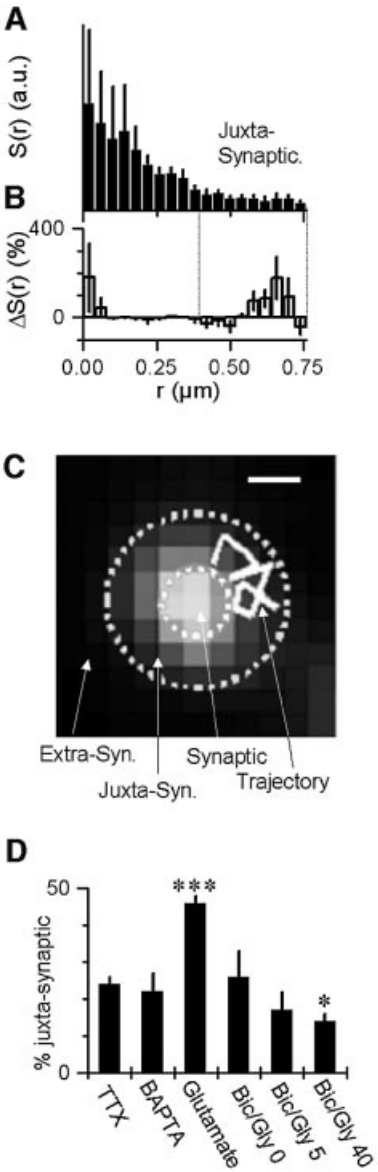

Fig. 6. Regulation of the topological distribution of extra-synaptic AMPARs in conditions of synaptic plasticity. (**A**) Surface proportion of the detected AMPARs, $S(r)$, as in Figure 1G, but in the presence of glutamate. (**B**) The difference (%) between Figure 1G and (D) reveals a significant increase of AMPARs in the presence of glutamate in an annulus ~400–800 nm from the center of the synapses defined later as the 'juxtasynaptic region'. (**C**) Example of a juxtasynaptic trajectory and of the different regions defined in the plasma membrane of the neurons with respect to synaptic staining. Scale bar = 500 nm. (**D**) Ratio of juxtasynaptic to extra-synaptic AMPARs in the six different conditions shown in Figures 4A and 5A. Glutamate-induced LTD doubles the proportion of juxtasynaptic AMPARs ($P < 0.001$ that the Glut value is different from the five others, Student's t-test) and a 40% decrease in the proportion of juxtasynaptic receptors after 40 min of Bic/Gly is found ($P < 0.05$ that the Bic/Glyc40 value is different from the five others, Student's t-test).

Discussion

Using single molecule imaging methods, we were able to image the movement of native AMPARs in synapses. The different behaviors of receptor movements both inside and outside synapses, as well as the topological distribution of the receptors in live neurons, could be sorted by studying over 5000 single molecule trajectories. We found that about half of synaptic receptors are mobile and that both the proportion and the amount of mobility are regulated by pharmacological treatments that modify receptor accumulation at synapses.

Individual fluorophores bear unique signatures, such as one-step photobleaching, well defined signals and diffraction-limited spots (Weiss, 1999). These allow us to ascertain that we were tracking single fluorescently tagged anti-GluR2 antibodies. Single molecule imaging can report receptor localization with 45 nm pointing accuracy (Schmidt *et al*., 1995; Thompson *et al*., 2002) and movement. First, in the extra-synaptic membrane, the presence of the antibody on the AMPARs will not *per se* modify receptor movements, as viscosity of the membrane and cytoplasm will by far dominate to limit diffusion. Secondly, the antibody itself did not promote aggregation of the receptors. However, the antibodies may report the movement of either individual or native clusters of receptors. We have no means of determining how many receptors would compose such native microaggregates, as both theoretical and experimental data have supported the notion that diffusion in a two-dimensional space is barely affected by the size of the diffusing object. This is exemplified by the fact that we observed comparable rates of free diffusion by single molecule imaging and tracking single receptor-bound 500 nm particles (Borgdorff and Choquet, 2002).

To identify synapses on live cells, we used FM1-43 and rhodamin 123 (see Materials and methods). These approaches correlate very well as both markers co-localized at ~80% in double staining experiments (data not shown). The density distribution of receptors, as seen by single molecule imaging, peaked at ~100 nm from the synapse center and decreased with a shallow slope toward the extra-synaptic membrane. Even though our distributions have a weaker resolution than electron microscopy data, it is interesting to note that we observed a enrichment of receptors roughly in the same range, although on the high end, as that observed with electron microscopy (Schikorski and Stevens, 1997; Takumi *et al*., 1999).

Antibody binding to AMPARs could potentially affect receptor movement in the synaptic cleft because of steric hindrance by extracellular molecules. This potential effect is difficult to appreciate. Indeed, on one hand the molecule density and arrangement in the synaptic cleft is not known. On the other hand, the size of the extracellular domain of AMPARs (Armstrong and Gouaux, 2000) is by itself rather large (~10 × 5 nm for one domain) and is comparable to that of an IgG molecule. In any case, our approach gives an upper limit on AMPAR mobility inside synapses.

Most receptors displayed Brownian movements outside synapses, as expected from freely diffusing receptors and previous studies (Borgdorff and Choquet, 2002). Mobile receptors inside synapses displayed a confined movement. This is a further indirect argument that molecules co-localized with presynaptic staining are indeed synaptic receptors. In synapses, receptor movements are confined to domains of mean radius 150 nm. This in good agreement with the reported size of PSDs as seen by electron microscopy (Schikorski and Stevens, 1997; Takumi *et al*.,

1999). The instantaneous diffusion of receptors in the domains was on average 0.06 $\mu m^2/s$, 5-fold lower than in the extra-synaptic membrane and 10 times higher than our experimental threshold for detection of mobile receptors. The reduction of receptor mobility and the process of confinement in synapses could have similar or different origins. Both are likely to arise from interactions with molecules present at high density in the PSDs (Scannevin and Huganir, 2000). These interactions could be either specific through short unresolved transient binding to associated scaffold molecules, or unspecific and leading to frictional slowing of the receptors. This is compatible with the observation that lowering temperature does not affect synaptic receptor diffusion. Confinement of receptors could also arise from corralling by permeable barriers present at the periphery of the PSD. In synapses, we also observed a large proportion of immobile receptors that are most likely bound to scaffold proteins acting as slots. Altogether, a unified picture of the postsynaptic density could be one where receptors are immobilized for transient periods of time related to the receptor–scaffold affinity. When unbound, receptors could diffuse in the space between slots at a relatively high rate and easily escape or re-enter the postsynaptic space. Trafficking of receptors in and out of synapses through lateral diffusion is likely to be a general phenomenon; NMDA receptors have been shown by electrophysiological recordings to exchange between synaptic and extra-synaptic sites through traffic in the plasma membrane (Tovar and Westbrook, 2002).

In single particle tracking studies, we had previously observed that receptor-bound particles stop reversibly at or near synapses (Borgdorff and Choquet, 2002). In those studies, the particle size (500 nm) prevented a more precise determination of the localization of immobilization sites. We show here that in the juxtasynaptic region diffusion properties are indistinguishable from those of other extra-synaptic receptors. Thus, the majority of sites of receptor immobilization are just in front of presynaptic terminals.

A number of protocols related to synaptic plasticity modify the accumulation of receptors at synapses. These modifications have mainly been viewed in the frame of regulation of endocytic and exocytic mechanisms. Here, we found that bath application of glutamate, which induces rapid depletion of AMPARs from synapses (Carroll *et al*., 1999b; Lissin *et al*., 1999), increases synaptic receptor diffusion rate, decreases the proportion of immobile synaptic receptors and increases the proportion of receptors in an area surrounding synapses. These results strongly suggest that glutamate-induced loss of postsynaptic receptors is due primarily to their escape from the PSDs through lateral diffusion. This would then be followed by their endocytosis in the extra-synaptic membrane. We have shown that endocytosed receptors are mainly immobile. That glutamate-induced endocytosed receptors are mainly concentrated in cell bodies (data not shown; Beattie *et al*., 2000) may explain why they escape our observation in neurites. Escape of AMPARs from the PSD could involve either the disruption of the postsynaptic actin cytoskeleton (Zhou *et al*., 2001) or a specific decrease in receptor affinity for a scaffold element. This would explain both the increased diffusion coefficient, by lowering the rate of fast transient binding of receptors to scaffold elements, and the decreased proportion of immobile receptors. The increase in the proportion of juxtasynaptic receptors in the presence of glutamate may correspond to receptors flowing out of the PSDs.

Inhibition of inhibitory neurotransmission together with potentiation of NMDARs activity, which results in increased surface expression of AMPARs (Lu *et al*., 2001; Passafaro *et al*., 2001), exhibit time-dependent effects on receptor mobility and localization. In the first minutes, there is mainly a decrease in the proportion of immobile synaptic receptors. After 40 min, both diffusion rates and percentage of immobile synaptic receptors are back to control values and the proportion of juxtasynaptic receptors is decreased. This observation relates to the fate of newly exocytosed AMPARs; using cleavable extracellular tags, it was observed that at early times after exocytosis, new GluR1 containing AMPARs are diffusively distributed along dendrites. This is followed by their lateral translocation and accumulation into synapses (Passafaro *et al*., 2001). GluR2 subunits were addressed directly at synapses. In our experiments, we followed the movement of native GluR2 containing AMPARs. They could also contain GluR1, -3 or -4, which could impose different trafficking behaviors (Malinow and Malenka, 2002). In any case, our data suggest that at the level of synapses themselves, newly added receptors are initially diffusive and then stabilized over time.

We found that the proportion of juxtasynaptic receptors varies inversely with the degree of receptor stabilization at the synapse. This supports the notion that the juxtasynaptic region around synapses represents not only a transit zone for receptors entering and leaving synapses through lateral diffusion, but also a reserve pool zone where receptors are available for recruitment at synapses. In this model, the pools of extra-synaptic and synaptic receptors are in a dynamic equilibrium. The degree of accumulation at the synapse would be set both by the total surface number of receptors and the residency time of the receptors in the synapse. It will be important to determine these times, which relate to the affinity of the receptors for the scaffold.

Materials and methods

Microscopy and single-molecule detection

An inverted microscope (Olympus IX70; Olympus, Bordeaux, France) equipped with a 100× oil-immersion objective (NA = 1.4) was used. Samples were illuminated for 30 ms at 633 nm by an He-Ne laser (JDS Uniphase, Manteca, CA) at a rate of 33 Hz. A defocusing lens permitted to illuminate a surface of $20 \times 20\ \mu m^2$ with an intensity of $7 \pm 1\ kW/cm^2$. A filter set (DCLP650, HQ575/50; Chroma Technology, Brattleboro, VT) permitted the detection of individual fluorophore by an intensified CCD camera (Pentamax Princeton Instruments, Trenton, NY). The total detection efficiency was ~5%. FM1-43 and rhodamine 123 were excited with the 488 nm line of an Ar^+ laser (Spectra Physics, Les Ulis, France) at an illuminating intensity of $2\ kW/cm^2$ using another filter set (DCLP498, Chroma Technology, and BA515, Omega Optical, Brattleboro, VT).

Cell culture, GluR2 and synapse staining

Hippocampal neurons from 18-day-old rat embryos were cultured on glass coverslips as described previously (Borgdorff and Choquet, 2002). For staining in TTX condition, neurons were incubated at 37°C (or 20°C) for 30 s with 5 μM FM1-43 (Molecular Probes, Eugene, OR) in culture medium supplemented with 40 mM KCl. They were then rinsed for 1 min in medium supplemented with 10 mM HEPES and 1 μM TTX (recording medium) before being incubated 10 min at 37°C (or 20°C) with 10 μg/ml anti-GluR2-Cy5 or anti-GluR2-Alexa647 (see Supplementary data). In control experiments, we verified that most FM1-43 staining disappeared

upon further depolarization by 40 mM KCl (not shown). In the two other conditions (see below), neurons were first incubated at 37°C for 5 min with 2 μM rhodamine 123. They were then fast-rinsed and incubated at room temperature for 10 min with the labeled antibodies. After fast rinses, the coverslips were mounted in a custom chamber with culture medium supplemented with 20 mM HEPES. The medium also contained either 1 μM TTX, 100 μM glutamate, or a combination of 20 μM Biccuculine, 1 μM strychnine and 200 μM glycine. For the BAPTA condition, neurons were first incubated with 5 μM BAPTA-AM at 37°C for 10 min before the antibody labeling, then rinsed at 37°C for 2 min and recorded in the presence of 1 μM TTX. All data were taken within 20 min after the last rinse. On a few occasions, we observed rapid (1 μm/s) movements of FM1-43 stains that we attributed to vesicle trafficking and were therefore discarded from our analysis. Rhodamine 123 concentrates in regions with high mitochondrial density such as presynaptic terminals. Specificity of the anti-GluR2 labeling was confirmed as virtually no staining was observed with the anti-GluR2 on several cell lines not expressing GluR2. We also verified by Trypan Blue exclusion that 15 min incubation with glutamate did not lead to immediate cell death (cell viability in control and glutamate conditions 74 ± 10%, $n = 20$ and 72 ± 14%, $n = 16$ fields, respectively; $n = 355$ and 209 neurons). For acid wash to remove surface labeling, live neurons were first labeled as above with anti-GluR2, incubated for 30 min at 37°C in culture medium and then washed for 2 min at 4°C in culture medium at pH 2 just before the experiment. Neurons were still metabolically active after this treatment as we could image normal intracellular transport of mitochondrias (data not shown).

For immunocytochemistry, neurons were incubated at 37 or 20°C with anti-GluR2 for 10 min. Neurons were then either fixed immediately with 4% PFA and sucrose or rinsed, maintained live for a further 15 min and then fixed and processed with secondary antibodies. For detection of surface and endocytosed receptors, fixed cells were first incubated for 45 min with 10 μg/ml secondary Alexa568 (Molecular Probes, Leiden, The Netherlands) anti-mouse antibody to saturate all surface bound anti-GluR2s. Saturation was verified in control experiments (not shown). Cells were then permeabilized and incubated for 45 min with 10 μg/ml secondary Alexa488 anti-mouse antibody to reveal endocytosed receptors. Green and red flurorescent images were quantified using metamorph (Universal Imaging, Downingtown, PA). The comparison of the levels of receptor clustering in live and fixed cells was measured as in Sergé *et al*. (2002).

Trajectory construction

The spatial distribution of the signals on the CCD originating from individual molecules was fitted to a two-dimensional Gaussian surface with a full-width at half-maximum of 360 ± 40 nm, given by the point-spread function of our apparatus. The two-dimensional trajectories of single molecules in the plane of focus were constructed by correlation analysis between consecutive images using a Vogel algorithm (Schuetz *et al*., 1997). Only trajectories containing at least three points were retained. This sets the minimum diffusion constant detectable with our setup, 7×10^{-3} μm²/s, which corresponds to the binning on the histograms. A systematic subtraction of 0.002 μm² is used to reject the bias induced by the pointing accuracy of the MSD.

Synaptic localization of AMPARs

The synaptic staining maxima (FM1-43 or rhodamine 123) were determined by fitting the fluorescence spots corresponding to presynaptic terminal with two dimensional Gaussians. The error on the fit was in the order of 60 nm. The distance from synapse center to a molecule was measured with a precision of ~80 nm, given the 45 nm pointing accuracy on molecules. The surfacic proportion, $S(r)$, is defined as the number of molecules detected between distances, r and $r + dr$, from the center of the nearest synapse divided by the total number of molecules and by the elementary surface of width dr. The results are shown in Figures 1G and 6D for steps $dr = 40$ nm and a mean neurite width of 1 μm (in a simple approximation, the elementary surface to take into account is equal to $2\pi rdr$ for $r < 500$ nm and constant for $r > 500$ nm).

Supplementary data

Supplementary data are available at *The EMBO Journal* Online.

Acknowledgements

We thank Philippe Ascher, Antoine Triller, Christophe Mulle and Thomas Schmidt for their comments on this manuscript, Michel Orrit for initiating this collaborative work and Laurent Groc for suggesting the acid wash experiment. We thank Dr El Mestikawy for the gift of the anti BNPI antibody. This work was supported by grants from the CNRS, the Conseil Régional d'Aquitaine, the Ministère de la Recherche and the European Community grant QLG3-CT-2001-02089.

References

Armstrong,N. and Gouaux,E. (2000) Mechanisms for activation and antagonism of an AMPA-sensitive glutamate receptor: crystal structures of the GluR2 ligand binding core. *Neuron*, **28**, 165–181.

Beattie,E.C., Carroll,R.C., Yu,X., Morishita,W., Yasuda,H., von Zastrow,M. and Malenka,R.C. (2000) Regulation of AMPA receptor endocytosis by a signaling mechanism shared with LTD. *Nat. Neurosci.*, **3**, 1291–1300.

Blanpied,T.A., Scott,D.B. and Ehlers,M.D. (2002) Dynamics and regulation of clathrin coats at specialized endocytic zones of dendrites and spines. *Neuron*, **36**, 435–449.

Borgdorff,A. and Choquet,D. (2002) Regulation of AMPA receptor lateral movement. *Nature*, **417**, 649–653.

Braithwaite,S.P., Meyer,G. and Henley,J.M. (2000) Interactions between AMPA receptors and intracellular proteins. *Neuropharmacology*, **39**, 919–930.

Carroll,R.C., Beattie,E.C., Xia,H., Luscher,C., Altschuler,Y., Nicoll,R.A., Malenka,R.C. and von Zastrow,M. (1999a) Dynamin-dependent endocytosis of ionotropic glutamate receptors. *Proc. Natl Acad. Sci. USA*, **96**, 14112–14117.

Carroll,R.C., Lissin,D.V., von Zastrow,M., Nicoll,R.A. and Malenka,R.C. (1999b) Rapid redistribution of glutamate receptors contributes to long-term depression in hippocampal cultures. *Nat. Neurosci.*, **2**, 454–460.

Carroll,R.C., Beattie,E.C., von Zastrow,M. and Malenka,R.C. (2001) Role of AMPA receptor endocytosis in synaptic plasticity. *Nat. Rev. Neurosci.*, **2**, 315–324.

Dickson,R.M., Norris,D.J., Tzeng,Y.L. and Moerner,W.E. (1996) Three-dimensional imaging of single molecules solvated in pores of poly(acrylamide) gels. *Science*, **274**, 966–969.

Dingledine,R., Borges,K., Bowie,D. and Traynelis,S.F. (1999) The glutamate receptor ion channels. *Pharmacol. Rev.*, **51**, 7–61.

Kusumi,A., Sako,Y. and Yamamoto,M. (1993) Confined lateral diffusion of membrane receptors as studied by single particle tracking (nanovid microscopy). Effects of calcium-induced differentiation in cultured epithelial cells. *Biophys. J.*, **65**, 2021–2040.

Lin,J.W., Ju,W., Foster,K., Lee,S.H., Ahmadian,G., Wyszynski,M., Wang,Y.T. and Sheng,M. (2000) Distinct molecular mechanisms and divergent endocytotic pathways of AMPA receptor internalization. *Nat. Neurosci.*, **3**, 1282–1290.

Lissin,D.V., Carroll,R.C., Nicoll,R.A., Malenka,R.C. and von Zastrow,M. (1999) Rapid, activation-induced redistribution of ionotropic glutamate receptors in cultured hippocampal neurons. *J. Neurosci.*, **19**, 1263–1272.

Lu,W., Man,H., Ju,W., Trimble,W.S., MacDonald,J.F. and Wang,Y.T. (2001) Activation of synaptic NMDA receptors induces membrane insertion of new AMPA receptors and LTP in cultured hippocampal neurons. *Neuron*, **29**, 243–254.

Luscher,C., Xia,H., Beattie,E.C., Carroll,R.C., von Zastrow,M., Malenka,R.C. and Nicoll,R.A. (1999) Role of AMPA receptor cycling in synaptic transmission and plasticity. *Neuron*, **24**, 649–658.

Malinow,R. and Malenka,R.C. (2002) AMPA receptor trafficking and synaptic plasticity. *Annu. Rev. Neurosci.*, **25**, 103–126.

Man,Y.H., Lin,J.W., Ju,W.H., Ahmadian,G., Liu,L., Becker,L.E., Sheng,M. and Wang,Y.T. (2000) Regulation of AMPA receptor-mediated synaptic transmission by clathrin-dependent receptor internalization. *Neuron*, **25**, 649–662.

Meier,J., Vannier,C., Sergé,A., Triller,A. and Choquet,D. (2001) Fast and reversible trapping of surface glycine receptors by gephyrin. *Nat. Neurosci.*, **4**, 253–260.

Moerner,W.E. and Orrit,M. (1999) Illuminating single molecules in condensed matter. *Science*, **283**, 1670–1676.

Noel,J., Ralph,G.S., Pickard,L., Williams,J., Molnar,E., Uney,J.B., Collingridge,G.L. and Henley,J.M. (1999) Surface expression of AMPA receptors in hippocampal neurons is regulated by an NSF-dependent mechanism. *Neuron*, **23**, 365–376.

Nusser,Z. (2000) AMPA and NMDA receptors: similarities and differences in their synaptic distribution. *Curr. Opin. Neurobiol.*, **10**, 337–341.

Passafaro,M., Piech,V. and Sheng,M. (2001) Subunit-specific temporal

and spatial patterns of AMPA receptor exocytosis in hippocampal neurons. *Nat. Neurosci.*, **4**, 917–926.
Scannevin,R.H. and Huganir,R.L. (2000) Postsynaptic organization and regulation of excitatory synapses. *Nat. Rev. Neurosci.*, **1**, 133–141.
Schikorski,T. and Stevens,C.F. (1997) Quantitative ultrastructural analysis of hippocampal excitatory synapses. *J. Neurosci.*, **17**, 5858–5867.
Schmidt,T., Schuetz,G.J., Baumgartner,W., Gruber,H.J. and Schindler,H. (1995) Characterization of photophysics and mobility of single molecules in a fluid lipid membrane. *J. Phys. Chem.*, **99**, 17662–17668.
Schnell,E., Sizemore,M., Karimzadegan,S., Chen,L., Bredt,D.S. and Nicoll,R.A. (2002) Direct interactions between PSD-95 and stargazin control synaptic AMPA receptor number. *Proc. Natl Acad. Sci. USA*, **99**, 13902–13907.
Schuetz,G.J., Schindler,H. and Schmidt,T. (1997) Single-molecule microscopy on model membranes reveals anomalous diffusion. *Biophys. J.*, **73**, 1073–1080.
Sergé,A., Fourgeaud,L., Hémar,A. and Choquet,D. (2002) Receptor activation and homer differentially control the lateral mobility of mGluR5 in the neuronal membrane. *J. Neurosci.*, **22**, 3910–3920.
Sheng,M. and Kim,M.J. (2002) Postsynaptic signaling and plasticity mechanisms. *Science*, **298**, 776–780.
Special Issue.(1999) Frontiers in chemistry: single molecules. *Science*, **283**, 1668–1695.
Takumi,Y., Ramirez-Leon,V., Laake,P., Rinvik,E. and Ottersen,O.P. (1999) Different modes of expression of AMPA and NMDA receptors in hippocampal synapses. *Nat. Neurosci.*, **2**, 618–624.
Thompson,R.E., Larson,D.R. and Webb,W.W. (2002) Precise nanometer localization analysis for individual fluorescent probes. *Biophys. J.*, **82**, 2775–2783.
Tovar,K.R. and Westbrook,G.L. (2002) Mobile NMDA receptors at hippocampal synapses. *Neuron*, **34**, 255–264.
Wang,Y.T. and Linden,D.J. (2000) Expression of cerebellar long-term depression requires postsynaptic clathrin-mediated endocytosis. *Neuron*, **25**, 635–647.
Weiss,S. (1999) Fluorescence spectroscopy of single biomolecules. *Science*, **283**, 1676–1683.
Zhou,Q., Xiao,M. and Nicoll,R.A. (2001) Contribution of cytoskeleton to the internalization of AMPA receptors. *Proc. Natl Acad. Sci. USA*, **98**, 1261–1266.

Received April 2, 2003; revised July 7, 2003;
accepted July 24, 2003